Dynamics of Composite Haldane Spin Chains in IPA-$CuCl_3$

T. Masuda,[1,*] A. Zheludev,[1,†] H. Manaka,[2] L.-P. Regnault,[3] J.-H. Chung,[4,‡] and Y. Qiu[4,‡]

[1]*Condensed Matter Science Division, Oak Ridge National Laboratory, Oak Ridge, Tennessee 37831-6393, USA*
[2]*Graduate School of Science and Engineering, Kagoshima University, Korimoto, Kagoshima 890-0065, Japan*
[3]*CEA-Grenoble, DRFMC-SPSMS-MDN, 17 rue des Martyrs, 38054 Grenoble Cedex 9, France*
[4]*NCNR, National Institute of Standards and Technology, Gaithersburg, Maryland 20899, USA*

(Received 5 November 2005; published 2 February 2006)

Magnetic excitations in the quasi-one-dimensional antiferromagnet IPA-$CuCl_3$ are studied by cold neutron inelastic scattering. Strongly dispersive gap excitations are observed. Contrary to previously proposed models, the system is best described as an asymmetric quantum spin ladder. The observed spectrum is interpreted in terms of composite Haldane spin chains. The key difference from actual $S = 1$ chains is a sharp cutoff of the single-magnon spectrum at a certain critical wave vector.

DOI: 10.1103/PhysRevLett.96.047210 PACS numbers: 75.10.Jm, 75.25.+z, 75.50.Ee

Antiferromagnetic 2-leg spin ($S = 1/2$) ladders and the closely related $S = 1$ Haldane spin chains [1,2] are an example of quantum disorder and mass generation in extended spin networks. In these *quantum spin liquids*, the magnetism is suppressed due to *collective* zero-point fluctuations and the unique topology of one dimension (1D), rather than to finite system size. Spin ladders play a key role in the dynamics of stripe phases in high-temperature superconductors [3] and under certain conditions can themselves support exotic types of superconductivity [4]. On a more fundamental level they are ideal models for studying the collective spin dynamics in 1D, quantum critical points and phase transitions in external magnetic fields, and the effects of quenched disorder.

Despite the wealth of relevant theoretical results, experimental studies are lagging behind because of a shortage of suitable model compounds. In the best known ladder examples $Sr_{14}Cu_{24}O_{41}$ [5] and $SrCu_2O_3$ [6] the large energy scales of magnetic interactions limit spectroscopic studies, especially at high fields. A typical problem with many known Haldane-gap systems [7,8] is a large single-ion magnetic anisotropy that is often associated with $S = 1$ spins, and qualitatively affects the dynamics and field behavior [9]. Moreover, a Haldane spin chain intrinsically has a smaller Hilbert space than $S = 1/2$ spin ladders, and therefore lacks certain very interesting spectral features [10]. In this Letter we report the discovery of an isotropic ladder spin network in the $S = 1/2$ compound $(CH_3)_2CHNH_3CuCl_3$ (IPA-$CuCl_3$), that was previously thought to be a prototypical ferromagnetic-antiferromagnetic (F-AF) spin chain [11]. We use inelastic neutron scattering to study its magnetic excitation spectrum. The experiments reveal a spectacular *truncation of the magnon branch* at certain critical wave vectors that we attributed to peculiarities of magnon interactions.

IPA-$CuCl_3$ crystallizes in a triclinic space group $P\bar{1}$ with $a = 7.766$ Å, $b = 9.705$ Å, $c = 6.083$ Å, $\alpha = 97.62°$, $\beta = 101.05°$, and $\gamma = 67.28°$ [11]. The key features of the structure are shown in Fig. 1. The magnetism is due to $S = 1/2$-carrying Cu^{2+} ions arranged in sheets parallel to the (a, c) crystallographic plane. These sheets are well separated by nonmagnetic organic layers. A spin gap of $\Delta \approx 1.5$ meV in IPA-$CuCl_3$ was first discovered by Manaka *et al.* [11] in $\chi(T)$ measurements. This value is consistent with the critical field $H_c \sim 11$ T that induces an ordered antiferromagnetic phase at low temperatures [12]. The gap was attributed to a singlet ground state of bond-alternating Cu^{2+} chains running along the crystallographic c axis, as shown by the dotted line in Fig. 1. Indeed, this model consistently explained all magnetization curves and ESR experiments, with a quantitative agreement obtained assuming alternating F-AF bonds [11]. An F coupling between nearest-neighbor Cu^{2+} sites $J_1 < 0$ [13] is consistent with the relevant Cu-Cl-Cu bond angles in the crystal structure of IPA-$CuCl_3$.

At the center of the present work are inelastic neutron scattering experiments on deuterated IPA-$CuCl_3$ samples, prepared by crystallization from solution [11]. The $\chi(T)$

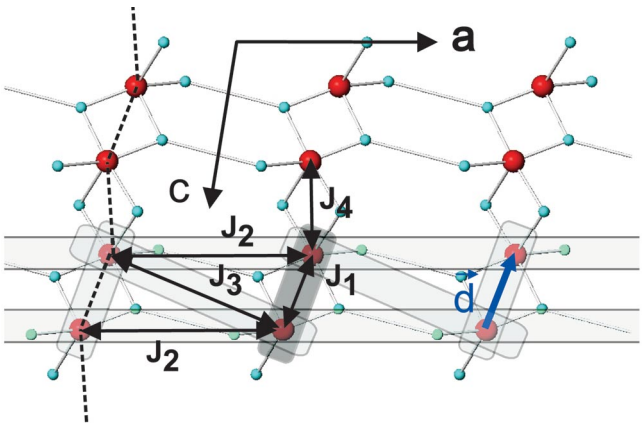

FIG. 1 (color). Layers of magnetic Cu^{2+} (red) and the bridging Cl^- ions (cyan) in IPA-$CuCl_3$. Previously proposed alternating Cu chains (dotted line) run along the c axis. Actual asymmetric spin ladders (shaded) are parallel to the a direction. The ladder rungs are defined by the vector **d**.

and ESR data for the deuterated samples agree well with those for the nondeuterated ones. Twenty single crystals with total mass of 3.5 g were coaligned to a mosaic spread of 4°. The data were collected using cold-neutron 3-axis spectrometers NG5-SPINS in NIST and IN12 in ILL, and at the Disc Chopper time-of-flight spectrometer (DCS) at NIST [14]. The sample was mounted with the (a, c) crystallographic plane parallel to the scattering plane of the instruments and maintained at or below $T = 1.5$ K. On SPINS we utilized (guide)—80'—80'—(open) collimations and a BeO filter after the sample for a fixed-final neutron energy $E_f = 3.7$ meV, selected by a flat pyrolitic graphite analyzer. On IN-12 a Soller collimator of 60' was used only at presample position. A Be filter was positioned after the sample. Neutrons of fixed-incident $E_i = 4.7$ meV or fixed-final $E_f = 3.5$ meV energies were used in conjunction with a horizontally focusing pyrolitic graphite analyzer. A constant background (typically 1.5 counts/min, depending on configuration) was subtracted from all 3-axis data sets. On the DCS instrument the data were taken with $E_i = 6.7$ meV neutrons, the incident beam forming an angle of 60° with the a^* direction. The background was directly measured by removing the sample from the cryostat.

A series of constant-E and constant-q scans revealed well-defined long-lived magnetic gap excitations in a large part of the Brillouin zone in IPA-$CuCl_3$. Typical data are shown in Fig. 2. Our measurements unambiguously show that the magnetic strong-coupling direction in IPA-$CuCl_3$ is along the crystallographic a axis. The global dispersion minimum is at $\mathbf{q} = (\frac{2n+1}{2}, 0, 0)$ with n integer [Fig. 3(a)], and also corresponds to a maximum of observed inelastic intensity. In contrast, the dispersion along the c^* axis is rather weak, with an energy minimum at $l = 0$ in Fig. 3(b). The originally proposed model of bond-alternating F-AF chains running along the crystallographic c axis is thus *totally inconsistent* with our results. Nevertheless, the measured gap energy $\Delta \sim 1.2$ meV is in agreement with that deduced from bulk measurements.

In the wave vector range $0.2 \leq h \leq 0.8$ and $1.2 \leq h \leq 1.8$, where sharp magnon peaks were observed, the 3-axis data were analyzed using a model single-mode (SM) cross section, with an empirical spin-gap dispersion relation [15], slightly modified to accommodate a transverse dispersion:

$$S(\mathbf{q}, \omega) \propto S^{\mathrm{SM}}(\mathbf{q})\delta(\omega - \omega_{\mathbf{q}}), \tag{1}$$

$$\omega_{\mathbf{q}}^2 = \omega_0^2\cos^2(\pi h) + [\Delta^2 + 4b_0^2\sin^2(\pi l)]\sin^2(\pi h) + c_0^2\sin^2(2\pi h), \tag{2}$$

where $\mathbf{q} = h\mathbf{a}^* + k\mathbf{b}^* + l\mathbf{c}^*$. The gap is equal to Δ at $l = 0$, and is allowed to slightly oscillate along c^* with a transverse bandwidth b_0. The boundary energy corresponds to ω_0. The cross section was numerically convoluted with the spectrometer resolution function calculated in the Popovici approximation [16] and fit to the experimental data. The magnetic form factor for Cu^{2+} ions was built into the fits. Separate coefficients $S^{\mathrm{SM}}(\mathbf{q})$ were used for each constant-$\mathbf{q}$ scan to determine the 3-dimensional structure factor in the most model-independent manner possible. The parameters of the dispersion relation in Eq. (2) were treated as global for all the collected scans. The fitting procedure yielded $\omega_0 = 4.08(9)$ meV, $\Delta = 1.17(1)$ meV, $b_0 = 0.67(1)$ meV, and $c_0 = 2.15(9)$ meV. Scans simulated using these parameter values are shown as shaded areas in Figs. 2(b)–2(d). The dispersion relations are plotted in solid lines in Fig. 3. Symbols in these plots were obtained in fits to individual scans, as opposed to global fits to the measured data. Figure 4(a) shows the l dependence of the single-mode component of the dynamic structure factor $S^{\mathrm{SM}}(\mathbf{q})$ measured at $h = 0.5$. The h depen-

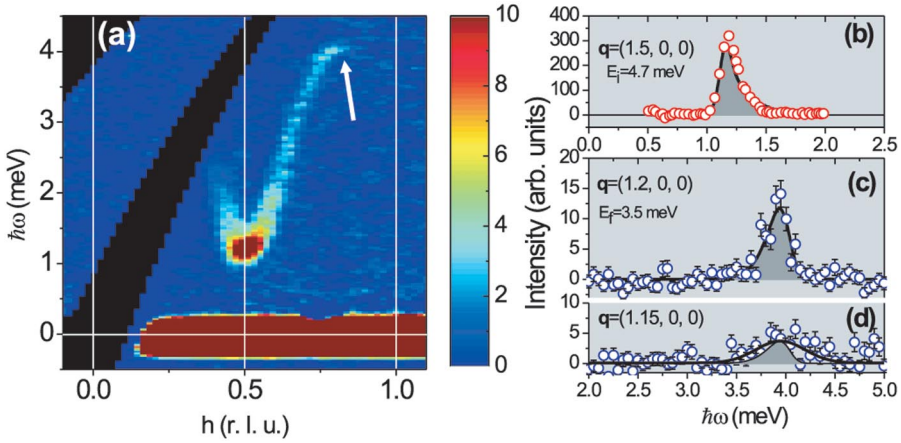

FIG. 2 (color). Time-of-flight (a) and 3-axis (b), (c), (d) inelastic neutron data measured in IPA-$CuCl_3$ at $T = 1.5$ K. The suppression of inelastic intensity at $h \leq 0.5$ in (a) is due to a large l (momentum transfer along c^*) and the FM-dimer structure factor for the magnon branch (see text). For $h > 0.5$, l is small at all times: $|l| < 0.2$. In (b), (c), (d) the shaded areas are calculated peak shapes due to resolution.

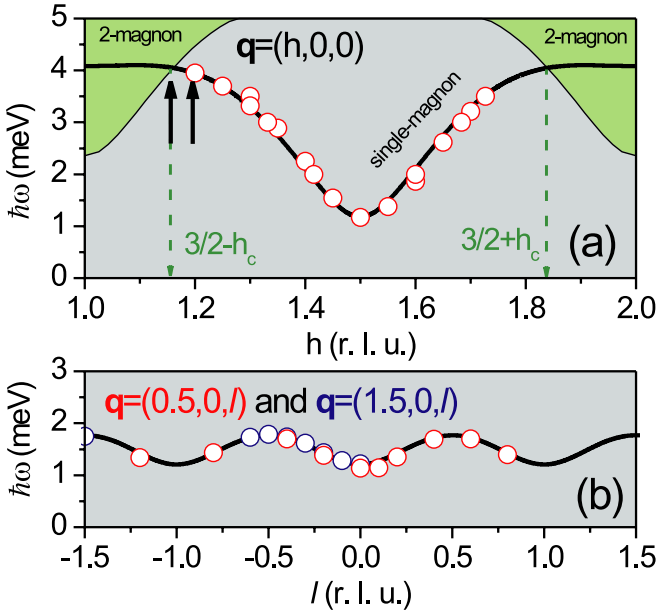

FIG. 3 (color online). Magnon dispersion measured in IPA-$CuCl_3$ along the a^* (a) and c^* (b) directions (symbols). Heavy solid lines are fits, as described in the text. In (a) the labeled shaded areas (green online) indicate the domain of the 2-magnon continuum. Solid arrows show the positions of scans in Figs. 2(c) and 2(d). Dashed arrows show the critical wave vectors.

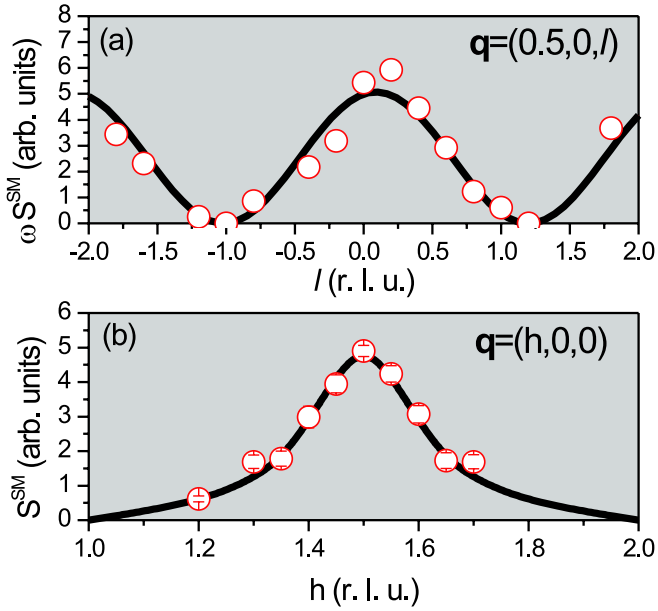

FIG. 4 (color online). Measured l (a) and h dependencies (b) of single-magnon excitation intensities in IPA-$CuCl_3$ (symbols). Solid lines are simulations, as described in the text.

dence of this structure factor for $l = 0$ is shown in Fig. 4(b).

The measured c-axis modulation of the magnon intensity is exactly explained by a ferromagnetic dimer with a particular spin separation $\mathbf{d}$ in the crystal structure (Fig. 1): $\mathbf{d} = (-0.0854, -0.1316, 0.4432)$. The data on the $h = \frac{2n+1}{2}$ reciprocal-space rods are very well reproduced by assuming $S^{\mathrm{SM}}(\mathbf{q}) \propto \cos^2(\pi h d_x + \pi l d_z)/\omega_{\mathbf{q}}$, as shown by the solid line in Fig. 4(a). To a good approximation one can thus describe IPA-$CuCl_3$ in terms of uniform chains made up of these ferromagnetically correlated spin pairs. The chains run along the crystallographic a axis and are composed of effective $S = 1$ spins. Since the single-mode intensity has its maximum at $h = \frac{2n+1}{2}$ [Fig. 4(b)], the correlations between the nearest-neighbor effective $S = 1$ spins are predominantly antiferromagnetic. If one assumes that near the magnetic zone center a dominant fraction of the total spectral weight is contained in the single-mode excitations, one can reproduce the measured h dependence of intensity with only nearest-neighbor AF interactions in the $S = 1$ chains. For this model $S(h) \propto \sin^2(\pi h)/\omega_h$, which is in good agreement with experiment [solid line in Fig. 4(b)]. We conclude that the singlet ground state in IPA-$CuCl_3$ and the gap excitations are due to *composite* $S = 1$ *Haldane spin chains* that run *perpendicular* to the originally proposed bond-alternating chains directions.

As shown in Fig. 1 the crystal structure of IPA-$CuCl_3$ presents a number of possible AF superexchange routes between Cu^{2+} spins along the a axis. In the most general case, the appropriate model for IPA-$CuCl_3$ is a *spin ladder* with F rung interactions J_1, a leg coupling constant J_2, and a diagonal exchange interaction of magnitude J_3 (presumably also AF). If this interaction were infinitely strong, the mapping onto a Haldane spin chain would be exact. In fact, the measured dispersion differs from that for an ideal $S = 1$ chain. In the latter, the ratio of the spin wave velocity v to the gap energy Δ is $v/\Delta \sim 6$ [17]. In contrast, in IPA-$CuCl_3$ $v/\Delta \approx 3.1$, about twice as small. The analogy with Haldane spin chains is thus only qualitative, and the $|J_1|$ is probably of the same order of magnitude as J_2 and J_3. Without a direct comparison with first-principle calculations, the exact values of the exchange constants can not be deduced from the measured dispersion and intensity modulation of the single-magnon excitations. The observed small dispersion of magnetic excitations along the c^* direction indicates a weak coupling J_4 between individual ladders (Fig. 1). From the position of the dispersion minimum we conclude that $J_4 < 0$.

A remarkable feature of the measured spectrum is the abrupt disappearance of the magnon branch at a certain critical wave vector q_c. This phenomenon is well illustrated by the time-of-flight data of Fig. 2(a). The sharp gap excitation extends to $h = \frac{1}{2} + h_c \sim 0.8$, where $h_c \sim 0.3$, and then vanishes abruptly, rather than persisting to the zone boundary at $h = 1$. Constant-q 3-axis data reveal similar behavior at the equivalent wave vector $h = \frac{3}{2} - h_c \sim 1.2$. The well-defined resolution-limited peak seen at $h = 1.2$ [Fig. 2(c)] is weakened and broadened at $h = 1.15$ [Fig. 2(d), where the shaded area is the simulated

profile for a resolution-limited peak], and is totally absent at $h = 1.1$ (not shown).

Such a dramatic *spectrum termination* phenomenon has been recently discovered and investigated in the quasi-2D material PHCC [18]. To our knowledge, IPA-$CuCl_3$ is the only other known spin-gap material with a similar feature. The effect can be explained by a coupling between single-magnon and multimagnon states [18–20]. The domain of the two-magnon continuum in IPA-$CuCl_3$, though invisible in our experiments due to low intensity and a very tight energy resolution, can be calculated using the measured one-magnon dispersion. As represented by the labeled (green online) shaded areas in Fig. 3(a), the continuum has a gap of 2Δ. Note that the single-magnon branch crosses into the 2-magnon continuum at exactly $h = \frac{2n+1}{2} \pm h_c$. Energy and momentum conservation laws forbid any single-magnon excitation *outside* the domain to decay into bunches of multiple magnons. For $\frac{2n+1}{2} - h_c < h < \frac{2n+1}{2} + h_c$ the magnons in IPA-$CuCl_3$ are thus stable. Their contribution to the dynamic structure factor are sharp δ-function peaks. This restriction is removed for magnons inside the continuum: they are rendered unstable through decaying into pairs of lower-energy magnons. Their energy width (inverse lifetime) is dramatically increased. In IPA-$CuCl_3$ this effect is particularly strong, and for $\frac{2n-1}{2} + h_c < h < \frac{2n+1}{2} - h_c$ there are no detectable single-magnon states.

What drives the decay process is interactions between magnons. Interestingly, in an ideal symmetric spin ladder the matrix elements between single-magnon and 2-magnon states are exactly zero, so the single mode survives inside the 2-magnon continuum [19,20]. In particular, in an isotropic Haldane spin chain stable magnons are expected to persist all the way to the zone-boundary. We can speculate that the abrupt disappearance of the magnon branch in IPA-$CuCl_3$, which distinguishes these composite Haldane spin chains from actual ones, is due to a symmetry-breaking diagonal interaction J_3.

Contrary to what was previously thought, IPA-$CuCl_3$ is a beautiful asymmetric spin ladder system, that for many purposes can be seen as a ''composite'' Haldane spin chain. Unlike an ideal Haldane spin chain, though, it features a spectacular end-of-spectrum effect at a certain critical wave vector. Future neutron work will focus on a direct observation of excitation continua, effects of high magnetic field, and Br-dilution.

We thank M. Stone, I. Zaliznyak, and M. Zhitomirsky for insightful discussions. S. Raymond is appreciated for his experimental support at ILL. Work at ORNL was carried out under Contract No. DE-AC05-00OR22725, US Department of Energy. T. M. was partially supported by the US - Japan Cooperative Research Program on Neutron Scattering between the US DOE and Japanese MEXT. The work at NIST is supported by the National Science Foundation under Agreements No. DMR-9986442, No. DMR-0086210, and No. DMR-0454672.

*Electronic address: tmasuda@yokohama-cu.ac.jp
Present address: International Graduate School of Arts and Sciences, Yokohama City University, 22-2, Seto, Kanazawa-ku, Yokohama city, Kanagawa, 236-0027, Japan.
†Electronic address: zheludevai@ornl.gov
Present address: Department of Materials Science and Engineering, University of Maryland, College Park, MD, 20742, USA.
‡Present address: Department of Materials Science and Engineering, University of Maryland, College Park, MD, 20742, USA.

[1] F. D. M. Haldane, Phys. Lett. **93A**, 464 (1983); Phys. Rev. Lett. **50**, 1153 (1983).
[2] S. R. White, Phys. Rev. B **53**, 52 (1996).
[3] J. M. Tranquada, H. Woo, T. G. Perring, H. Goka, G. D. Gu, M. Fujita, and K. Yamada, Nature (London) **429**, 534 (2004).
[4] M. Uehara, T. Nagata, J. Akimitsu, H. Takahashi, N. Môri, and K. Kinoshita, J. Phys. Soc. Jpn. **65**, 2764 (1996).
[5] M. Matsuda, K. Katsumata, H. Eisaki, N. Motoyama, S. Uchida, S. M. Shapiro, and G. Shirane, Phys. Rev. B **54**, 12 199 (1996).
[6] M. Azuma, Z. Hiroi, M. Takano, K. Ishida, and Y. Kitaoka, Phys. Rev. Lett. **73**, 3463 (1994).
[7] L. P. Regnault, I. Zaliznyak, J. P. Renard, and C. Vettier, Phys. Rev. B **50**, 9174 (1994).
[8] A. Zheludev, Y. Chen, C. L. Broholm, Z. Honda, and K. Katsumata, Phys. Rev. B **63**, 104410 (2001).
[9] A. Zheludev *et al.*, Phys. Rev. Lett. **88**, 077206 (2002); Phys. Rev. B **68**, 134438 (2003); **69**, 054414 (2004).
[10] O. P. Sushkov and V. N. Kotov, Phys. Rev. Lett. **81**, 1941 (1998).
[11] H. Manaka, I. Yamada, and K. Yamaguchi, J. Phys. Soc. Jpn. **66**, 564 (1997).
[12] H. Manaka, I. Yamada, Z. Honda, H. A. Katori, and K. Katsumata, J. Phys. Soc. Jpn. **67**, 3913 (1998).
[13] In our definition $J > 0$ corresponds to AF interactions. The 2-spin Hamiltonian is written as $+J\mathbf{S}_1\mathbf{S}_2$. Note that Refs. [11,12] use a different convention: $J > 0$ corresponds to ferromagnetism and the exchange term is $-J\mathbf{S}_1\mathbf{S}_2$.
[14] J. R. D. Copley and J. C. Cook, Chem. Phys. **292**, 477 (2003).
[15] T. Barnes and J. Riera, Phys. Rev. B **50**, 6817 (1994).
[16] M. Popovici, Acta Crystallogr. Sect. A **A31**, 507 (1975); M. Popovici, D. Stoica, and I. ionita, J. Appl. Crystallogr. **20**, 90 (1987).
[17] E. S. Sørensen and I. Affleck, Phys. Rev. B **49**, 15 771 (1994).
[18] M. B. Stone, I. A. Zaliznyak, T. Hong, C. L. Broholm, and D. H. Reich, cond-mat/0511266.
[19] M. E. Zhitomirsky (private communication).
[20] A. Kolezhuk and S. Sachdev, cond-mat/0511353.